

# NUMERICAL ANALYSIS OF THE SUBMERGED INDUCTION HARDENING PROCESS

Alexandru SPAHIU, Virgiliu FIREȚEANU

POLITEHNICA University of Bucharest, EPM\_NM Laboratory  
313 Splaiul Independentei, 77206, Bucharest, Romania  
tel/fax: (+40) 21.411.65.58

e-mail: [s\\_alexandru@amotion.pub.ro](mailto:s_alexandru@amotion.pub.ro), [Virgiliu.Fireteanu@electro.masuri.pub.ro](mailto:Virgiliu.Fireteanu@electro.masuri.pub.ro)

*Abstract – This article deals with the study of the submerged induction hardening process. The paper performs a numerical analysis of the heating and cooling stage of two hardening processes. A hardening process uses the induction submerged heating technique, and the other hardening process uses the air induction heating technique. These processes are simulated by means of a quasi 1D model and a 2D model.*

## INTRODUCTION

The submerged induction heating is used in tooth-by-tooth induction hardening process in order to produce a continuous hardened layer, which extends along the entire length of the gears teeth [1].

The goal of the paper is to carry out a numerical analysis of the submerged induction hardening process. For that, there are used two finite elements models in order to highlight the advantages and drawbacks of this hardening technique.

Thus, are used two computation domains: a quasi 1D domain and a 2D domain. By means of the quasi 1D model, it is studied the influence of the frequency and of the surface density of induced power on the austenized depth and on the heating time. The 2D model results contain a thermal study: the evolution of the billet temperature during the hardening process and a metallurgical one: the microhardness profile obtained at the end of the process.

For a better accuracy of the magneto-thermal numerical results, the temperature dependence of all physical properties and the magnetic non-linearity of the workpiece are considered. The metallurgical characteristics influencing the local values of hardness at the end of the process are defined by the quantities austenized depth and hardened depth [2][3].

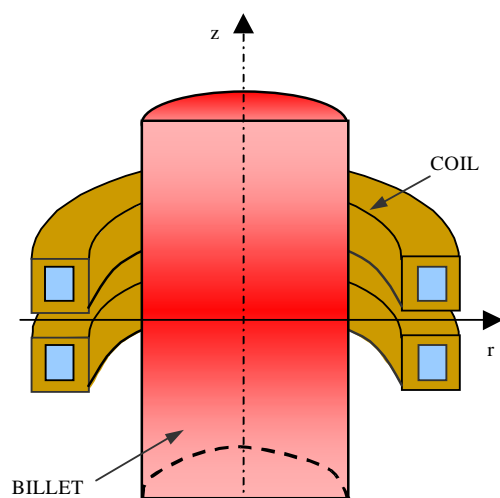


**Fig. 1.** Physical model of the hardening process

## PHYSICAL MODEL

The physical model deals with the induction heating stage, followed by the cooling process of a cylindrical steel workpiece. The outline of the assembly workpiece – inductor is shown in Fig. 1.

The billet having the diameter  $d_2 = 60$  mm is placed into an axial A.C. magnetic field with the frequency taking three values: 4 kHz, 10 kHz and 400 kHz.

The geometry of the physical model contains a two-turn coil having the outer dimensions 10 x 10 mm (height x width) of the copper tube conductor.

The current in the coil is the source of the electromagnetic field. The rms value of the current is time independent; consequently, the circuit associated to the field problem contains an ideal current source that supplies the coil.

The value of the current in the simulations of induction heating for the quasi 1D domain is established by successive tests for each set of frequency values, in order to cover the 0.5 – 6 kW/cm<sup>2</sup> range of surface density of induced power.

The austenized depth  $\Delta_a$  [2] is evaluated in steady state regime, considering the value  $\theta_a = 800$  °C of the austenization temperature. In case of scanning induction hardening, this dimension characterizes the point of maximum penetration inside the billet of the isotherm  $\theta(r, z) = \theta_a$ .

All the physical properties of the billet material are temperature dependent as described in [2].

### NUMERICAL MODELS

The two computation domains take into account the symmetries of the physical model. Thus, they are reduced to a quarter of the entire assembly. These two computation domains and their mesh are presented in Fig 2 and Fig 3.

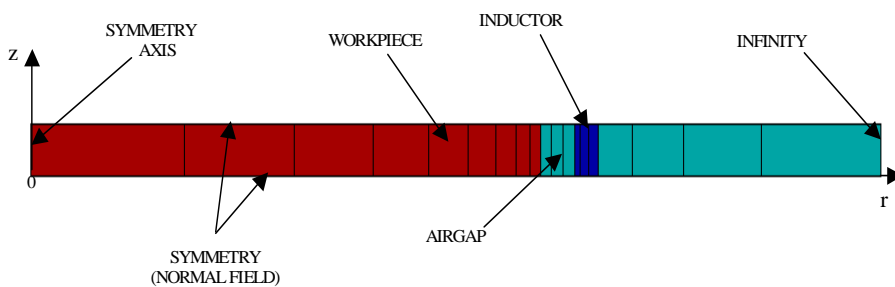


Fig.2. Computation domain of the quasi 1D model

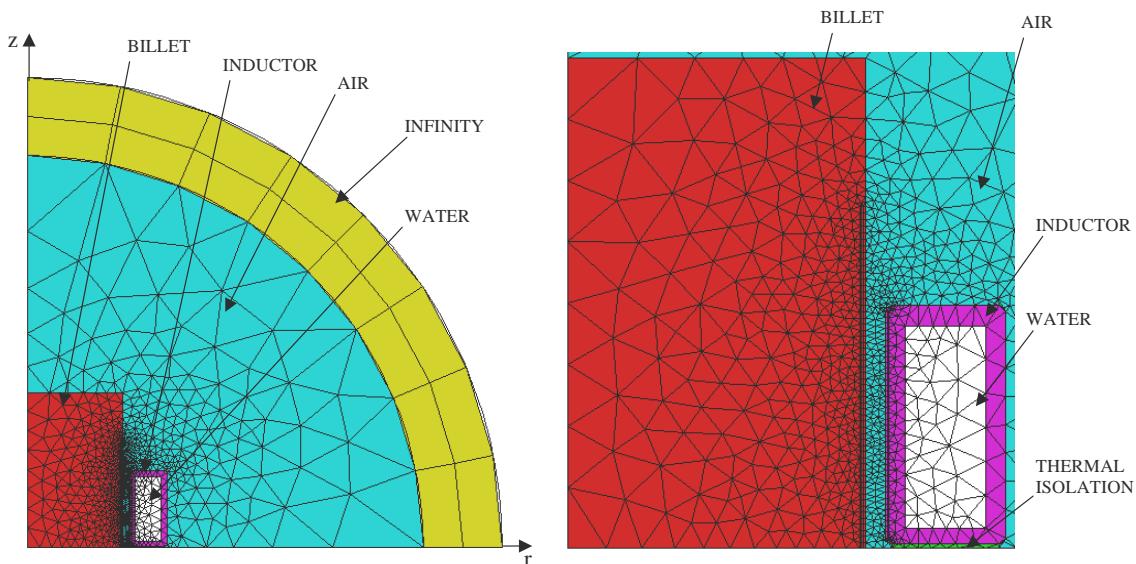


Fig.3. Computation domain of the 2D model

### MATHEMATICAL MODELS OF MAGNETO-THERMAL COUPLING

The electromagnetic field is expressed in complex vector magnetic potential  $\underline{\mathbf{A}}(r, z)$  and has azimuthal orientation in the entire computation domain. The transient temperature field  $\theta(r, z, t)$  is considered in the billet region. The coupling of these two fields is expressed by the equations:

$$j\omega\sigma\underline{\mathbf{A}} + \text{curl} (1/\mu \text{curl} \underline{\mathbf{A}}) = \underline{\mathbf{J}}_1 \tag{1}$$

$$\rho C_p d\theta / dt + \text{div}(k \text{grad}\theta) = p_j = \omega^2\sigma|\underline{\mathbf{A}}|^2 \tag{2}$$

where:  $\omega = 2\pi f$ ,  $\sigma$  stands for the electric conductivity,  $\mu$  for magnetic permeability,  $\underline{J}_1$  for current density in the inductor, source of electromagnetic field. In the second equation, which characterizes the transient heating of the billet region,  $\rho C_p$  is the specific heat capacity,  $k$  is the thermal conductivity and  $p_j$  is the induced power density, source of thermal field.

**RESULTS – HEATING SIMULATION**

The transient heating of the billet is presented in the charts of billet temperature at different time steps, Fig. 4, when the maximal values of billet temperature are 800, 900, 1000, 1100 and 1200 °C.

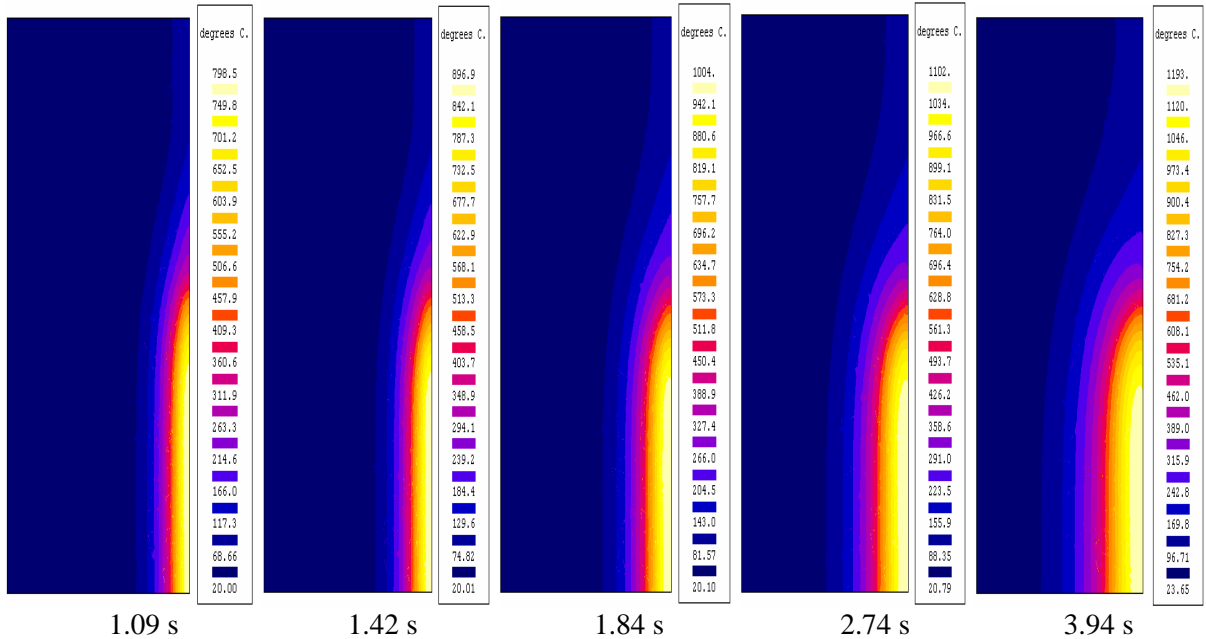


**Fig. 4.** Evolution of billet temperature during the submerged heating process

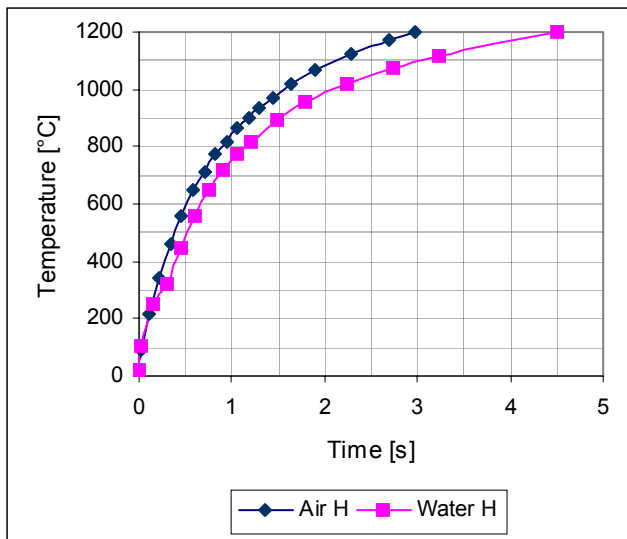


**Fig. 5.** Time variation of the surface billet temperature during the heating process

The time variation of the temperature in the point placed to the half of the billet surface ( $r = 30 \text{ mm}$ ,  $z = 0 \text{ mm}$ ) is represented in Fig.5.

We observe that for the same surface temperature of the billet and for identical value of supply current, the heating time is superior for submerged application than for air heating.

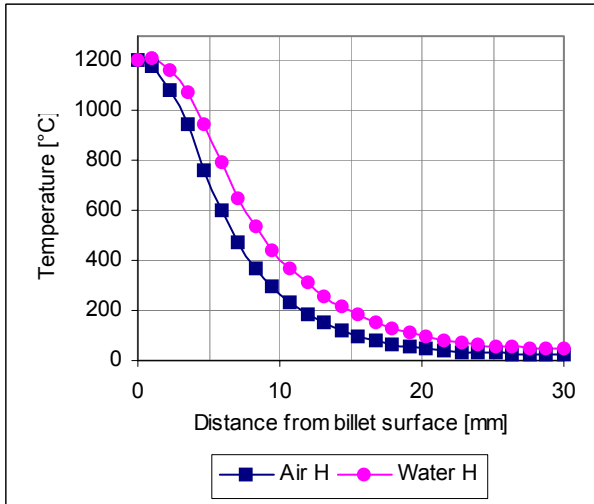


Fig. 6 shows that the austenized depth, distance measured from the billet surface where the temperature is higher than austenization temperature, it is also higher for the submerged heating than for air heating.

**Fig. 6.** Temperature variation with distance from billet surface at the end of the heating

### DEPENDENCIES OF AUSTENIZED DEPTH ON FREQUENCY AND SURFACE DENSITY OF INDUCED POWER

Numerical values of the specific surface power  $p_s$  and of the heating time  $t_h$  are obtained by post-processing the simulation results of quasi 1D application.

Corresponding to the heating of the workpiece surface up to the temperature  $\theta_{smax} = 1200\text{ }^\circ\text{C}$ , the dependence of austenized depth on frequency and on surface density of induced power is shown in the Fig. 7.

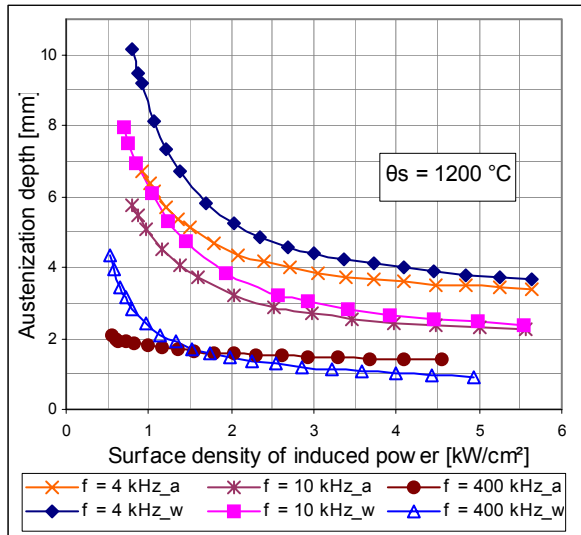


**Fig. 7.** Dependence of austenized depth on frequency and on surface density of induced power

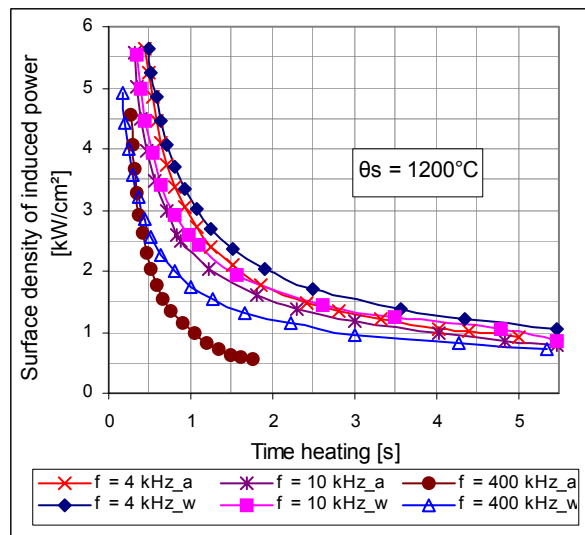


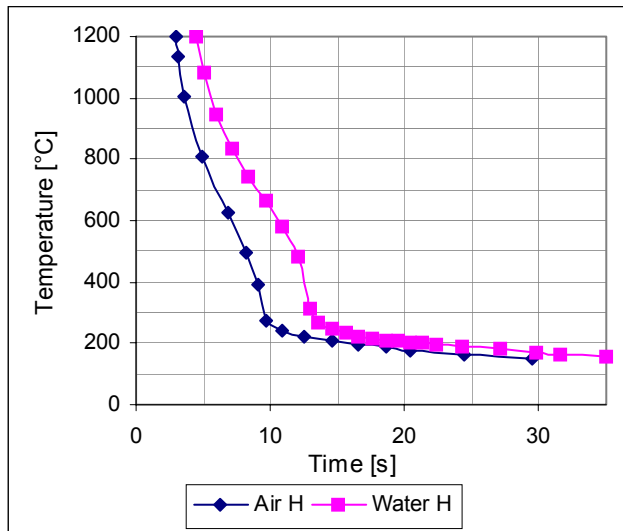
**Fig. 8.** Dependence of surface density of induced power on frequency and on heating time

Another important parameter is the heating time. The dependence of surface density of induced power on heating time is presented in the Fig. 8

It must be mentioned that in the legend, the series names is composed by a number that represent the frequency followed by the letter *a* or *w*. The letter represents the abbreviation of air, respectively water, the heating media.

## RESULTS – COOLING SIMULATION

In Fig. 9 is presented the temperature variation during the cooling process. The cooling agent is the water whose dependence of heat convection coefficient on temperature is given in [4].



We observe that the cooling rate is higher in the case of air heating than for submerged heating. This is due to the superior heat quantity stored in the billet in the case of submerged heating.

As result of the workpiece cooling, Fig. 10 contains the variation of hardness versus distance from billet surface at the end of the hardening process. The more rapid cooling of the air heating process results in a superior value for the hardness.

**Fig. 9.** Time variation of the temperature of billet surface during the cooling process

The variation of hardness in case of submerged heating shows a good uniformity of the hardened layer. Also the thickness of this layer is higher, as predicted from Fig. 6 and according with [3].

The chart of hardened layer is shown in Fig. 11 that emphasizes previously remarks.

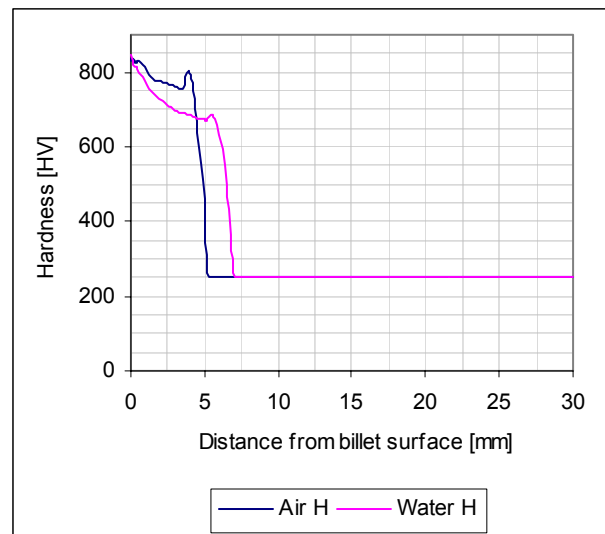


**Fig. 10.** Variation of hardness versus distance from billet surface

## CONCLUSIONS

The numerical analysis of the phenomena characterizing the induction hardening takes into consideration the magnetic non-linearity of the workpiece and the temperature dependence of all physical properties.

Based on simulation results of the induction heating and of the cooling process, this paper carried out a comparison between the specific parameters of the submerged heating, respectively air heating stages of a hardening process.

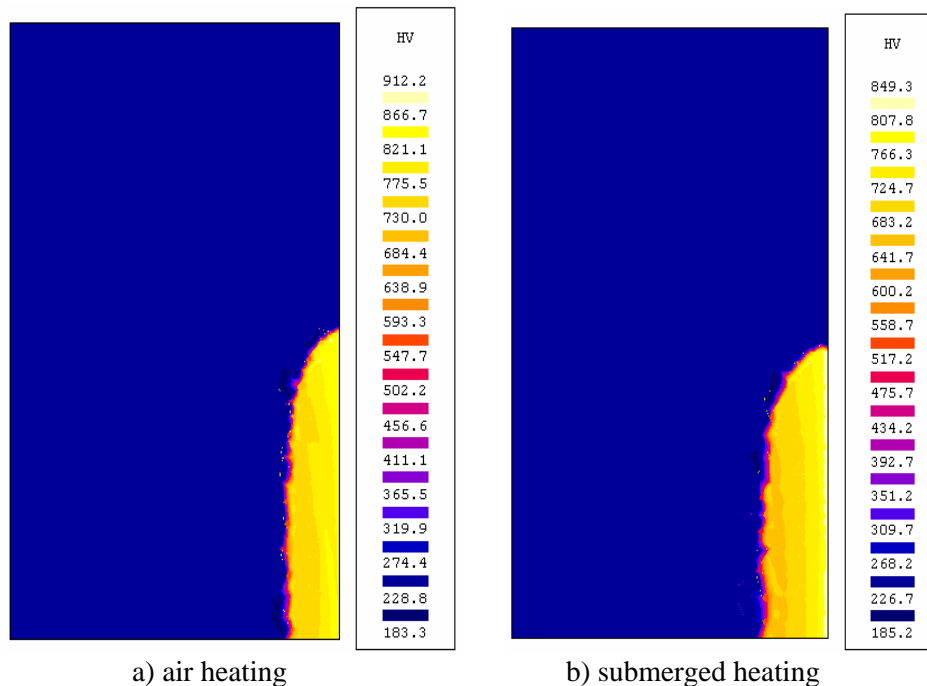


Fig. 10. Charts of the hardness at the end of the cooling process

Comparing the numerical results of the heating stage is obtained a superior heating time and a higher value of austenized depth for the submerged process than for the air heating process. The analysis of the billet microhardness at the end of the cooling stage shows that the air heating process assures superior values of the billet hardness. Instead, the billet hardened by the submerged process has a superior value for the hardened layer that also is more uniform.

## REFERENCES

- [1] G. Parrish, D.W. Ingham and M. Chaney: "The submerged induction hardening of gears", Heat treatment of metals, 1998
- [2] J. I. Asperheim, V. Fireteanu, S. T. Hagen, A. Spahiu and T. Tudorache: "Nomographs for induction hardening, using the numerical simulation of induction heating", in *Proceedings of OPTIM'2000 Conference*, Brasov, Romania
- [3] A. Spahiu and V. Fireteanu: "Austenized Depth and Hardened Depth - Two Criteria for Induction Hardening Characterization", in *Proceedings of 48. Internationales Wissenschaftliches Kolloquium Technische Universität Ilmenau*
- [4] Mitelea I., Budau V.: "Metals Handbook" (*Studiul Metalelor*), FACLA Press, Timisoara, 1987 (in romanian language)
- [5] Prisma: *Metal7 User Guide*, 2001
- [6] Cedrat - Recherche: *FLUX2D User Guide*, 2002,
- [7] Ericsson T: "Principles of Heat Treating of Steels", ASM Handbook, Vol 4 – Heat Treating, 10<sup>th</sup> Edition.
- [8] J. Furhmann, D. Homberg and M. Uhle: "Numerical Simulation of Induction Hardening of Steel", in *Proceedings of 8<sup>th</sup> IGTE Symposium*, Graz (1998).
- [9] Bates Ch., Totten G., Brennan R.: "Quenching of Steel", ASM Handbook, Vol 4 – Heat Treating, 10<sup>th</sup> Edition.
- [10] M. Swierkosz, O. Greim and D. Mari: "Numerical Simulation of Induction Heating and Thermal Treatment of Metals", in *Proceedings of EPM'1997*, Paris.